

# ON FACILITATED OXYGEN DIFFUSION IN MUSCLE TISSUES

JOHN E. FLETCHER, *Laboratory of Applied Studies, Division of Computer  
Research and Technology, National Institutes of Health, Bethesda, Maryland  
20205 U.S.A.*

**ABSTRACT** The role of myoglobin in facilitated diffusion of oxygen in muscle is examined in a tissue model that utilizes a central supplying capillary and a tissue cylinder concentric with the central capillary, and that includes the nonlinear characteristics of the oxygen-hemoglobin dissociation reaction. In contrast to previous work, this model exhibits the effect of blood flow and a realistic, though ideal, tissue-capillary geometry. Solutions of the model equations are obtained by a singular-perturbation technique, and numerical results are discussed for model parameters of physiologic interest. In contrast to the findings of Murray, Rubinow, Taylor, and others, fractional order perturbation terms obtained for the "boundary-layer" regions near the supplying capillaries are quite significant in the overall interpretation of the modeling results. Some closed solutions are found for special cases, and these are contrasted with the full singular-perturbation solution. Interpretations are given for parameters of physiologic interest.

## INTRODUCTION

The concept of a moving, carrier-mediated transport, of which myoglobin-facilitated oxygen diffusion is an outstanding example, has stimulated the interest of both experimental and theoretical investigators since the early 1920's. Roughton, in a 1932 paper, suggested a facilitation contribution by the hemoglobin to oxygen transport within the red cell (1). Further interest in the importance of this effect was generated by the research review of Millikan in 1939 (2), and was followed by the work of Klug et al. (3, 4), who during this period conducted theoretical investigations in parallel with laboratory experiments.

The interest in myoglobin, an intracellular oxygen-binding heme protein, arises from its broad occurrence in mammalian muscle tissue with two different but related functional roles. For example, the muscles of deep diving mammals such as seals are dark red because of their

---

Editor's note: This paper is the first sent to the Biophysical Journal as *computer ready copy* and represents a successful experiment in a scientific journal's use of computer age publication.

After its acceptance, this paper was sent by Dr. Fletcher to the printer with a copy on magnetic tape which was fed directly to a typesetting computer. The computer program to translate the data file on the National Institutes of Health (NIH) Wylbur text editor to a form compatible with the typesetter was originally written by Bonnie Douglas and developed by Bonnie Douglas and Martha Horton of the Laboratory of Applied Studies (LAS) Division of Computer Research and Technology (DCRT), NIH. The format calls were inserted by Nancy Crawford of the Physical Sciences Laboratory, DCRT, NIH.

I am grateful for support and cooperation from Dr. Fletcher and Dr. Eugene Harris of LAS, our publisher, The Rockefeller University Press, and our printer, Science Press, in performing this experiment in data transmission. I hope, with the many new forms of electronic text-editing used by our authors, that it will soon be possible to avoid retyping manuscripts at the printing plant by submission on magnetic media and to enjoy the advantages of speed, cost, and accuracy characteristic of modern information transfer.

rich, oxygenated myoglobin content. Here, the tissue myoglobin functions primarily as a long-term oxygen store for use during the dive when the oxygen supply is cut off. In birds, myoglobin is believed to act as a short-term store, particularly in the wings and hearts, for muscles that carry out rhythmic contractions in which the blood supply is reduced during contraction and replenished upon relaxation (5).

In other land dwelling animals, the functional role of myoglobin is unclear. For example, in man myoglobin occurs as ~1.4% of dry weight in the heart, and ~2.5% of skeletal muscle. The resting metabolic rate of skeletal muscle is  $\sim 5 \times 10^{-8}$  mol  $O_2$ /cm<sup>3</sup> live tissue/s. Myoglobin contains a single binding site for oxygen and at normal concentrations can store  $\sim 3 \times 10^{-7}$  mol  $O_2$ /cm<sup>3</sup> of live tissue. The maximal oxygen reserve provided by the saturated myoglobin stores is therefore  $3 \times 10^{-7} / 5 \times 10^{-8} = 6$  s. Clearly, the storage or reserve function of myoglobin would not appear to justify its occurrence. One therefore expects an additional functional role for the myoglobin, such as a facilitator of oxygen transport within the tissues. The experimental and analytical work thus far suggests that myoglobin in the higher mammals could indeed act as a carrier or facilitator of oxygen transport, in addition to its role as a limited oxygen store (2, 6, 7).

In 1959 and 1960 Wittenberg (7) and Scholander (8) independently studied the effects of myoglobin in mammalian muscle. They both showed that the oxygen flux depended on the initial concentration of the carrier molecule in the solution. Wyman is credited with the derivation of the basic theoretical model; most investigators use the reaction-diffusion equations as described by Wyman in his 1966 paper (9).

Wittenberg, in a 1970 paper (10), has given an extensive review of the existing experimental data, the conjectures on the role of myoglobin, a discussion of alternative mechanisms, and a summary of the existing theoretical modeling analyses. Kreuzer and Hoofd have studied the flux of oxygen through hemoglobin solutions and have treated the describing equations numerically (11, 12). Their computed results were in excellent agreement with experimental findings. In addition, they have collected and reviewed the available numerical values for the parameters in the theoretical models.

Kreuzer (12), Murray (13), and Smith et al. (14) have been active in the theoretical modeling of facilitated diffusion in the chemical engineering literature. Extensions of the mathematical techniques used in these papers have been considered by Rubinow and Dembo (15). These various theoretical studies and experimental inquiries span the period from 1970 to the present.

The modeling efforts to date generally have not made attempts to consider actual or idealized microcirculatory geometry. In addition, no paper has included blood flow or blood hemoglobin dissociation kinetics in the transport, even for the description of steady-state models. Some attempts to use a realistic geometry are found in the recent papers of Murray (16), Taylor and Murray (17), and Van Ouwkerk (18). However, these papers assume a uniform, nonflowing oxygen concentration source external to an infinitely long, solid tissue cylinder, which is clearly a nonphysiologic idealization. Thus, while the previous models are useful for gaining insight into laboratory experiments, carrier facilitation concepts, and techniques for the solution of the theoretical equations, they have not contributed directly to an examination of the functional role of facilitation in actual or ideal tissue structures. We present here a model and results that represent extensions of the previous work to include

realistic, though idealized, microcirculatory geometry, constant blood flow and blood-oxygen kinetics, and a finite capillary length. This description of facilitated oxygen diffusion should reflect the transport contribution of myoglobin in mammalian striated muscle tissue.

## FORMULATION OF THE MODEL

The approach often used in modeling of myoglobin facilitation is to consider a one-dimensional slab or solution of protein with fixed boundary concentration or flux boundary conditions. Such a model can be realized in an experimental laboratory design, and modeling results are comparable with experimentally obtained values (9–11, 13). In *in situ* muscle tissues, however, one finds a quite different geometrical arrangement of blood and tissue. In general, muscle fibers are long, cylindrically shaped units, with each fiber bundle having capillaries parallel to and surrounding each fiber (19–21). Oxygen-rich blood enters these capillaries from the supplying arterioles, flows along parallel to the muscle fibers, giving up its oxygen as it transits the capillary, and exits into the venules as oxygen-deficient blood. Clearly, the factors of blood flow, local hemoglobin saturation, and tissue metabolic demand for oxygen determine the local oxygen concentration at the muscle fiber surface. It is also clear that this concentration is nonconstant from the arteriolar to venous ends of the capillary. Such a model of tissue substrate supply has been described (22), and we modify it here to include the effect of a binding protein in the tissue space. A geometric idealization of this arrangement is shown in Fig. 1.

In using a single cylinder of fixed length and radius, one must keep in mind that the results can represent only an average condition, which is the mean over a distribution of capillary lengths and radii. The objective here is to determine if myoglobin facilitation can play a significant role in tissue oxygen supply. The model results will not represent the true oxygen concentration at any fixed point in an actual tissue, but should represent the mean conditions in a typical tissue structure. This model will be referred to as a Krogh cylinder, or tissue cylinder, in the remainder of this paper.

The concept of enhanced transport from whole blood to tissue myoglobin to tissue respiration is illustrated schematically in Fig. 2. The lower curve is the blood-oxygen saturation curve, the middle curve is the oxygen-myoglobin saturation curve, and the upper

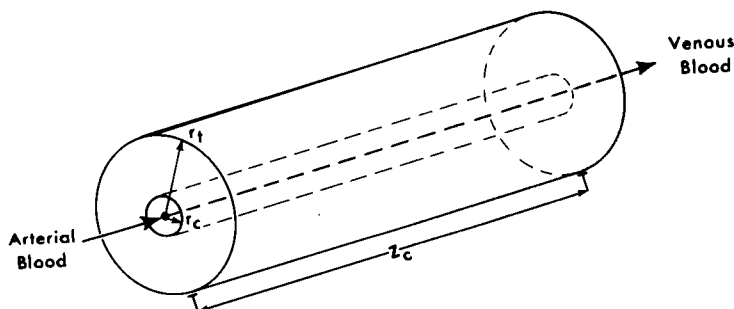


FIGURE 1 The Krogh cylinder model.  $r_t$  is the outer tissue radius,  $r_c$  is the capillary radius, and  $l_c$  is the axial length of the central capillary and its surrounding tissue cylinder.

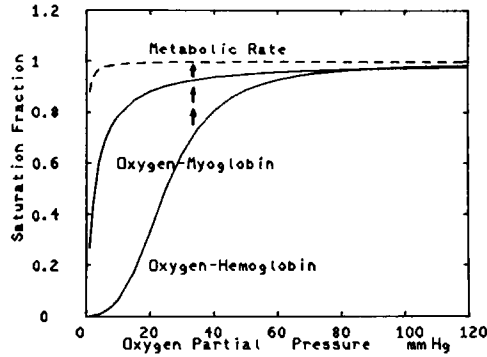


FIGURE 2 The transport relationship of hemoglobin to myoglobin to respiratory pigments in the consuming tissues. The figure is illustrative, and is not intended to quantitate the actual substrate transfer.

curve is the cellular metabolic rate of tissue. The direction of oxygen transfer is represented by the arrows.

It seems well established that the principal mechanism of facilitation within the tissues is molecular diffusion (9, 10), and for the limited purposes of this paper, the oxygen states in the idealized tissue domain can be described by a system of nonlinearly coupled reaction-diffusion equations that describe the steady-state (time-independent) conditions of tissue respiration. The details of model development can be found elsewhere, and we simply list here the relevant equations (9, 10, 19, 22).

#### MATHEMATICAL MODEL OF TISSUE AND CAPILLARY BLOOD

We use the mass-action equation, as do Wyman (9) and others, to describe the combination of myoglobin and oxygen in the tissue. This is symbolically,



The local kinetic reaction rate  $\rho$  in tissue is described by

$$\rho(Y, P_t) = c_p[k_1 s_t(1 - Y)P_t - k_2 Y], \quad (2)$$

where  $Y$  is the fraction of myoglobin saturated with oxygen,  $P_t$  is the partial pressure of oxygen in tissue,  $s_t$  is the solubility of oxygen in tissue,  $c_p$  is the tissue concentration of myoglobin,  $k_1$  is the rate of association of myoglobin and oxygen, and  $k_2$  is the rate of disassociation of oxymyoglobin. In the tissue domain

$$\begin{aligned} \frac{1}{r} \frac{\partial}{\partial r} \left( r s_t D_o \frac{\partial P_t}{\partial r} \right) &= \rho(Y, P_t) + Q(P_t) \\ c_p \frac{1}{r} \frac{\partial}{\partial r} \left( r D_m \frac{\partial Y}{\partial r} \right) &= -\rho(Y, P_t) \end{aligned} \quad (3)$$

where  $r$  is the radial coordinate from capillary center,  $z$  is the axial coordinate along capillary axis,  $D_o$  is the oxygen diffusion coefficient in tissue,  $D_m$  is the oxymyoglobin diffusion

coefficient in tissue, and  $Q(P_t)$  is the respiration rate in resting tissue. The boundary conditions for the tissue equations are the natural conditions at the capillary-tissue interface

$$\begin{aligned} P_t(r_c, z) &= P_b(z) \quad (\text{continuity of pressure}), \\ P_b(0) &= P_A \quad (\text{capillary entrance pressure}), \\ \frac{\partial Y}{\partial r}(r_c, z) &= 0 \quad (\text{zero oxyhemoglobin flux}); \end{aligned} \quad (4)$$

and the tissue cylinder outer symmetry conditions

$$\begin{aligned} \frac{\partial P_t}{\partial x}(r_t, z) &= 0 \quad (\text{symmetry of oxygen partial pressure}), \\ \frac{\partial Y}{\partial x}(r_t, z) &= 0 \quad (\text{symmetry of oxyhemoglobin fraction}), \end{aligned} \quad (5)$$

where  $P_b$  is the partial pressure of oxygen in capillary blood,  $P_A$  is the partial pressure of oxygen in arteriolar blood,  $r_c$  is the radius of the central capillary, and  $r_t$  is the radius of the tissue cylinder.

An idealized model of steady-state capillary blood is obtained by a mass balance with the average tissue flux conditions and the assumption of thermodynamic equilibrium of the capillary blood. The resulting implicit equation is

$$s_b v_o \frac{d}{dz} [P_b + \alpha H(P_b)] = \frac{2}{r_c} s_t D_o \frac{\partial P_t}{\partial r} \bigg|_{r=r_c}, \quad (6)$$

where  $H(P) = (1/4)P(d/dP) \ln(1 + A_1 P + A_2 P^2 + A_3 P^3 + A_4 P^4)$  is the oxygen-hemoglobin dissociation function (Adair equation),  $\alpha = C/s_b$ ,  $C$  is the whole blood capacity for oxygen,  $s_b$  is the solubility of oxygen in capillary blood, and  $v_o$  is the flow velocity of whole blood in a capillary.

The tissue equations (Eqs. 3) are similar to those considered by Wyman (9), Murray (13), and others, but the blood-tissue geometrical arrangement and therefore the boundary conditions are quite different in this application. We must seek a solution that couples the capillary equation (Eq. 6) to the tissue equations (Eqs. 3) through the capillary wall interface conditions (Eq. 4).

#### DIRECT INTEGRATION OF MODEL EQUATIONS

The technique used to solve the model equations follows lines similar to earlier procedures described by Wyman (9) and later, Murray (13). Adding Eqs. 3, we eliminate the nonlinear reaction rate  $\rho$  to obtain

$$\frac{1}{r} \frac{\partial}{\partial r} \left( r s_t D_o \frac{\partial P_t}{\partial r} + c_p r D_m \frac{\partial Y}{\partial r} \right) = Q(P_t). \quad (7)$$

The oxygen metabolic rate  $Q(P_t)$ , in general, will depend on the local oxygen partial pressure. This dependence has been expressed as a Michaelis-Menten form, as described in reference 17. However, this function remains nearly constant at oxygen pressures above 1–2 mmHg, as

shown in Fig. 2. Therefore, we shall assume for purposes of this investigation that the tissue metabolic rate  $Q(P_t)$  can be taken as the constant  $K$ . In fact, muscle metabolism is known to continue by anaerobic glycolysis in the absence of oxygen. This phenomena is known as the accumulation of the "oxygen-debt."

Setting  $Q(p_t) = K$ , and using the boundary conditions (Eqs. 5) at  $r = r_t$ , a first integral of Eq. 7 is

$$s_t D_o r \frac{\partial P_t}{\partial r} + c_p D_m r \frac{\partial Y}{\partial r} = -\frac{K}{2} (r_t^2 - r^2). \quad (8)$$

Evaluating Eq. 8 at  $r = r_c$  and using the third of Eqs. 4 we determine

$$\frac{2}{r_c} s_t D_o \frac{\partial P_t}{\partial r} \bigg|_{r=r_c} = -K\Omega, \quad (9)$$

where  $\Omega = (r_t/r_c)^2 - 1$  and is always positive.

Eq. 9 can be used directly in Eq. 6, and uncouples it from the tissue equations. The uncoupling permits the direct integration of the capillary equation, since the right side is now independent of axial variable  $z$  and radial variable  $r$ .

By using the second of Eqs. 5, an implicit expression for  $P_b(z)$  is obtained by direct integration of Eq. 6. This is

$$P_b(z) - P_A + \alpha[H(P_b) - H(P_A)] = -\frac{K}{v_o s_b} \Omega z. \quad (10)$$

Note that the capillary partial pressure depends only on the geometry involved and the tissue demand for oxygen. This is a direct result of the assumption that tissue metabolic demand is independent of the local oxygen pressure.

$P_b(z)$  is now implicitly determined and can be obtained by an inversion of Eq. 10 for each value of  $z$ . A second integral of the combined diffusion equations (Eqs. 8), and the use of the first of boundary conditions (Eqs. 4) yields the tissue space solution

$$P_t(r, z) - \frac{c_p D_m}{s_t D_o} [Y_o(z) - Y(r, z)] = P_b(z) - \frac{K r_t^2}{2 D_o s_t} \left[ \ln \left( \frac{r}{r_c} \right) - \frac{1}{2} \left[ \left( \frac{r}{r_t} \right)^2 - \left( \frac{r_c}{r_t} \right)^2 \right] \right]. \quad (11)$$

This equation contains the unknown dependent functions  $P_t(r, z)$ ,  $Y_o(z)$ , and  $Y(r, z)$ , and requires additional functional relationships to independently resolve all the unknowns. However, some insight can be gained by a direct examination of the components of Eqs. 10 and 11.

#### A DISCUSSION OF THE IMPLICIT RELATIONSHIPS

It is clear from the form of Eq. 10 that a closed implicit relationship involving the capillary oxygen partial pressure  $P_b(t)$ , the hemoglobin saturation fraction  $H(P_b)$ , the tissue metabolic rate  $K$ , and the various geometric parameters has been obtained. Clearly, Eq. 10 can be solved implicitly for  $P_b(z)$  to yield the blood-tissue interface pressure as a function of capillary axis position. This function is then used as the boundary data,  $P_b(z)$ , for the tissue equation (Eq. 11).

An inspection of Eq. 11 reveals some properties of the function of the tissue myoglobin. That the nature of the contribution of myoglobin to steady-state tissue oxygen levels can be identified at this point seems to have been overlooked in many previous analytical treatments. It is clear from physical considerations that the saturation fraction of myoglobin at the capillary-tissue interface is higher than at any interior point, i.e.,  $Y_o(z) \geq Y(r, z)$ . Therefore the oxymyoglobin component  $c_p D_m / s_i D_o [Y_o(z) - Y(r, z)]$  is always nonnegative. Consider now the remaining quantities on the right in Eq. 11. We define the functions

$$F(r, z) = Y_o(z) - Y(r, z)$$

$$P_o(r, z) = P_b(z) - \frac{K r_i^2}{2 D_o s_i} \left[ \ln \left( \frac{r}{r_c} \right) - \frac{1}{2} \left[ \left( \frac{r}{r_i} \right)^2 - \left( \frac{r_c}{r_i} \right)^2 \right] \right], \quad (12)$$

where  $F(r, z)$  is the net tissue oxymyoglobin radial desaturation and  $P_o(r, z)$  is the nonfacilitated oxygen pressure in tissue and is the well known Krogh-Erlang solution for the steady-state Krogh cylinder with no myoglobin present to facilitate oxygen supply (19, 22). The facilitated oxygen partial pressure in tissue is the sum

$$P_t(r, z) = G \cdot F(r, z) + P_o(r, z), \text{ where } G = \frac{c_p D_m}{s_i D_o}. \quad (13)$$

In this sense, the facilitated increase in tissue oxygen partial pressure is a direct addition to the transport by linear diffusion.

#### THE KINETIC EQUILIBRIUM SOLUTION

Although Eqs. 10 and 11 represent closed implicit expressions for the facilitation effects in tissue, neither  $Y_o(z)$  nor  $Y(r, z)$  are explicitly known. Therefore, a complete solution is not available without additional assumptions relating  $Y_o$ ,  $Y$ , and  $P_t$ ; or, one solves the second of Eqs. 3 with  $P_t$  eliminated as a dependent variable. We consider an additional assumption first, and use the resulting solution as a standard against which a singular perturbation solution of Eqs. 3 can be compared.

Since the kinetic equations are quite "stiff," the oxymyoglobin saturation fraction is expected to be very near the equilibrium value.<sup>1</sup> Thus, if one assumes that the oxygen-myoglobin reaction is always at equilibrium, it is not necessary to solve the oxymyoglobin radial diffusion equation, since the oxymyoglobin saturation is then completely determined by the local oxygen partial pressure. By definition of kinetic equilibrium,  $\rho(Y, P_t) = 0$ , and using Eq. 2,

$$Y(r, z) = \frac{\delta P_t(r, z)}{\gamma + \delta P_t(r, z)}, \text{ and } Y_o(z) = \frac{\delta P_b(z)}{\gamma + \delta P_b(z)}, \quad (14)$$

where  $\delta = s_i k_1$  and  $\gamma = k_2$ , and  $P_t(r_c, z) = P_b(z)$ . These relationships can be used directly in

<sup>1</sup>Stiffness in the sense used here means that the solution will behave like  $y = y_s + (y_o - y_s) \exp [-\beta(t - t_o)]$ , where  $\beta$  is a large positive number. Clearly, the solution is always driven back to the equilibrium value  $y_s$  by any departure  $y_o - y_s$  from equilibrium. This is the result of a large coefficient  $\beta$  in an equation of the form  $dy/dt = \beta(y_s - y)$ , with  $y(t_o) = y_o$ .

Eq. 13 to obtain a single closed implicit equation for  $P_i$ . This is

$$P_i(r, z) + G \frac{\delta P_i(r, z)}{\gamma + \delta P_i(r, z)} = G \cdot Y_o(z) + P_o(r, z). \quad (15)$$

This equation is quadratic in  $P_i$  and can be inverted for the unique positive function. The positive solution of Eq. 15 is given by

$$P_i(r, z) = P_o(r, z) + \frac{1}{2\delta} \left( \{[\gamma - \delta G(1 - Y_o(z)) + \delta P_o(r, z)]^2 + 4G\delta\}^{1/2} - [\gamma + \delta G(1 - Y_o(z)) + \delta P_o(r, z)] \right). \quad (16)$$

Note that the quantity in large parentheses in Eq. 16 is always positive so that the facilitated pressure  $P_i$  always exceeds the linear diffusion pressure  $P_o$ . This will be discussed more fully later.

Since the reaction kinetics are neglected, we expect the saturation fraction values for this solution to be slightly higher than the nonequilibrium values. This is shown to be the case by direct comparison with a singular perturbation solution for the nonequilibrium case. A numerical comparison for parameters of physiologic interest is given in Table I and is discussed in some detail in the Results section.

TABLE I  
A COMPARISON OF NONEQUILIBRIUM AND KINETIC EQUILIBRIUM SOLUTIONS

$x$	Myoglobin saturation			Oxygen partial pressure		
	PS	ES	$\Delta Y_o$	PS	ES	$\Delta P$
	(%)			(mmHg)		
0.10	91.36	91.72	-0.36	22.68	22.68	0.00
0.12	90.96	91.02	-0.06	20.71	20.76	-0.05
0.14	90.32	90.35	-0.03	19.10	19.16	-0.06
0.16	89.66	89.68	-0.02	17.74	17.80	-0.06
0.18	89.01	89.03	-0.02	16.55	16.61	-0.06
0.20	88.36	88.38	-0.02	15.52	15.58	-0.06
0.22	87.72	87.74	-0.02	14.60	14.66	-0.06
0.24	87.09	87.11	-0.02	13.77	13.83	-0.06
0.26	86.46	86.48	-0.02	13.03	13.09	-0.06
0.28	85.84	85.86	-0.02	12.37	12.43	-0.06
0.30	85.22	85.24	-0.02	11.76	11.82	-0.06
0.40	82.22	82.24	-0.02	9.42	9.48	-0.06
0.50	79.49	79.51	-0.02	7.88	7.94	-0.06
0.60	77.14	77.16	-0.02	6.85	6.91	-0.06
0.70	75.26	75.28	-0.02	6.17	6.23	-0.06
0.80	73.92	73.94	-0.02	5.75	5.81	-0.06
0.90	73.13	73.15	-0.02	5.52	5.58	-0.06
1.00	72.87	72.89	-0.02	5.44	5.50	-0.06

A numerical comparison of the equilibrium solution (ES) and the perturbation solution (PS) for facilitated oxygen diffusion. The model parameters are for the standard reference case and the values are for a radial profile at the venous end,  $y = 1.0$  or  $z = z_c$ , of the capillary. This is the location of the greatest differences in the solutions.  $D_m = 0.7 \times 10^{-6}$ ,  $c_p = 5.0 \times 10^{-7}$ , and  $D_o = 1.5 \times 10^{-5}$ .



## THE SINGULAR PERTURBATION PROBLEM

The functions defined by Eqs. 12 can be used to eliminate  $P_i$  as a dependent variable in the second of Eqs. 3 and to thereby obtain a single equation for the radial desaturation variable  $F(r, z)$ . For convenience, we also define the free myoglobin fraction

$$U(z) = 1 - Y_o(z). \quad (17)$$

$U(z)$  represents the fraction of deoxygenated, free, myoglobin at the capillary-tissue interface. The diffusion equation for the radial desaturation variable  $F$  then becomes

$$c_p \frac{1}{r} \frac{\partial}{\partial r} \left( r D_m \frac{\partial F}{\partial r} \right) = c_p \{ k_1 s_t [U(z) + F] P_t + k_2 [U(z) + F] - k_2 \}. \quad (18)$$

This equation will have the boundary conditions

$$\begin{aligned} F(r_c, z) &= 0; \\ \frac{\partial F}{\partial r}(r_c, z) &= 0; \\ \frac{\partial F}{\partial r}(r_t, z) &= 0. \end{aligned} \quad (19)$$

Note that  $U(z)$  is an unknown coefficient function to be determined. That  $U(z)$  is an unknown coefficient function, and the observation that the numerical values of the parameters in the model are large, lead us to consider Eqs. 18 and 19 as a singular perturbation problem. Note that we have an overdetermined system, i.e., a second-order differential equation with three boundary conditions.

To pose Eq. 18 as a singular perturbation problem, it is more convenient to work with a normalized form of the equation and the associated boundary conditions (Eqs. 19). We introduce the nondimensional space variables

$$x = r/r_t, \quad x_c = r_c/r_t, \quad y = z/z_c \quad (20)$$

and the perturbation parameter  $\epsilon$  in the range

$$0 \leq \epsilon \leq 10^{-4}. \quad (21)$$

These new variables suggest the nondimensional system parameters

$$\begin{aligned} a &= \epsilon \frac{c_p k_1 r_t^2}{D_o} \sim O(1) \\ b &= \epsilon \frac{s_t k_1 r_t^2}{D_p} \sim O(1) \\ c &= \epsilon \frac{k_2 r_t^2}{D_p} \sim O(1) \\ \psi &= \frac{K r_t^2}{2 D_o s_t} \left( \frac{1}{x_c} - x_c \right) \sim O(1). \end{aligned} \quad (22)$$

The nondimensional facilitation equation to be considered as a singular perturbation problem then becomes

$$\epsilon \frac{1}{x} \frac{\partial}{\partial x} \left( x \frac{\partial F}{\partial x} \right) = aF^2 + [aU(y) + bP_o(x, y) + c]F + U(y)[bP_o(x, y) + c] - c; \quad (23)$$

with the boundary conditions

$$\begin{aligned} F(x_c, y) &= 0, \\ \frac{\partial F}{\partial x}(x_c, y) &= 0, \\ \frac{\partial F}{\partial x}(1, y) &= 0. \end{aligned} \quad (24)$$

### THE ZERO-ORDER SOLUTION

The perturbation techniques used to solve Eqs. 23 with Eqs. 24 are similar to methods used by Wyman (9), Murray (13), and Meldon et al. (14), although the model treated here requires a different analysis and technique at the respective boundaries. In general, we seek an expansion in  $\epsilon$  for the deoxygenation variable

$$F(x, y) = F_o(x, y) + \epsilon^\sigma F_\sigma(x, y) + \epsilon^\tau F_\tau(x, y) + \dots, \quad (25)$$

where the real exponents  $\sigma, \tau, \dots$  are to be determined and the terms in the expansion are obtained by satisfying the differential equation (Eq. 18) for monotonically increasing exponents of the perturbation parameter  $\epsilon$ . Letting  $\epsilon \rightarrow 0$ , the differential equation (Eq. 23) reduces to the algebraic equation

$$aF^2 + [aU(y) + bP_o(x, y) + c]F + U(y)[bP_o(x, y) + c] - c = 0. \quad (26)$$

As it stands, Eq. 26 cannot be solved since the coefficient function  $U(y)$  is unknown. However, we can obtain a zero-order (in  $\epsilon$ ) approximation for  $U(y)$  by evaluating Eq. 26 at  $x = x_c$ , then solving for  $U(y)$ . Using the first boundary condition  $F(x_c, y) = 0$ ,

$$U(y) = \frac{c}{c + bP_o(x_c, y)}, \text{ or } Y_o(y) = \frac{bP_o(x_c, y)}{c + bP_o(x_c, y)}. \quad (27)$$

The quantity  $U(y)$  represents the unsaturated myoglobin fraction at the capillary tissue interface and  $Y_o(y) = 1.0 - U(y)$  is the saturated fraction. Note that the zero-order approximation produces the kinetic equilibrium solution (Eq. 14) for  $Y_o(y)$ , since in the normalized variables  $P_o(x_c, y) = P_b(y) = P_b(z)$ . This equivalence is clear if one observes that  $c/b = \gamma/\delta$ ; so that  $Y_o(z) = [bP_o(x_c, y)]/[c + bP_o(x_c, y)] = [\delta P_b(z)]/[\gamma + \delta P_b(z)]$ .

With a zero-order determination of  $U(y)$  now available, Eq. 26 can be solved to zero order for the deoxygenation variable  $F(x, y)$ . The zero-order positive solution for  $F(x, y)$  becomes

$$F(x, y) = ([\xi(x, y) - aU(y)]^2 + 4ac)^{1/2} - [\xi(x, y) + aU(y)]/2a, \quad (28)$$

where  $\xi(x, y) = bP_o(x, y) + c$ .

This solution can be recognized as the facilitation part of the kinetic equilibrium solution (Eq. 16) if we use the equivalences  $a/b = G$ ,  $c/b = \gamma/\delta$ , and  $c/a = (\gamma/\delta)(1/G)$ .

It is then clear that the zero-order perturbation solution has real physical meaning, in addition to being the low-order approximation to the complete nonequilibrium solution. This result also suggests that the dynamic state of the nonequilibrium solution is represented by the higher-order terms and cannot be inferred from the zero-order solution.

Unlike Murray's solutions for the infinite cylinder, the solution (Eq. 28) does not satisfy all of the boundary conditions given by Eqs. 24. The first condition was imposed by our choice of  $U(y)$ ; but, differentiating Eq. 28, we see that

$$\frac{\partial F}{\partial x}(x_c, y) = \frac{bc}{ac + \xi^2(x_c, y)} \psi, \text{ and } \frac{\partial F}{\partial x}(1, y) = 0. \quad (29)$$

Therefore, the zero-order solution satisfies the first and third of boundary conditions (Eqs. 24), but not the second. This implies that the neglected terms, assumed to be of higher order in amplitude, have first derivatives of zero order. Thus, higher-order terms must be considered to completely satisfy all the boundary conditions. This is to be expected, since the flux rates and diffusion of the oxymyoglobin are intimately related to the neglected terms in Eq. 23.

#### THE BOUNDARY-LAYER EQUATIONS

As constructed, the solution of the algebraic equation (Eq. 26) yields the kinetic equilibrium solution (Eq. 16), but this solution does not reflect the dynamics of the derivative terms, especially near the capillary-tissue interface. Physically speaking, the "layer" near the capillary-tissue interface is a region in which a rapid exchange of free and oxygenated myoglobin is occurring. The dynamics of this process are, of course, reflected in the derivative terms that were neglected in the construction of the zero-order solution. A determination of the fractional exponents and a detailed discussion of the "boundary-layer contribution" is given in Appendix I. Suffice it to say here that we assume expansions in  $\epsilon$  of the form

$$\begin{aligned} F(x, y) &= F_0(x, y) + \epsilon^{1/2} F_{1/2}(x, y) + \epsilon F_1(x, y) + \dots \\ U(y) &= U_0(y) + \epsilon^{1/2} U_{1/2}(y) + \epsilon U_1(y) + \dots, \end{aligned} \quad (30)$$

which can be shown to be of the correct order. These expansions and the local coordinate transformation  $\mu = (x - x_c)\epsilon^{-1/2}$  lead directly to the "boundary-layer" equation

$$\frac{d^2 F_{1/2}}{d\mu^2} - \omega^2 F_{1/2} = U_{1/2}(y) \xi(x_c, y). \quad (31)$$

The initial data for this equation is

$$\begin{aligned} F_{1/2}(0) &= 0 \\ \frac{dF_{1/2}}{d\mu}(0) &= \frac{-bc}{ac + \xi^2(x_c, y)} \psi \end{aligned} \quad (32)$$

where  $\omega^2 = aU_0(y) + \xi(x_c, y)$ . In obtaining this equation, we have neglected all terms of order

$\epsilon$  and higher, and have used the properties of  $F_o(x, y)$  near  $x = x_c$ . The differential equation contains the unknown coefficient function  $U_{1/2}(y)$ , which can be regarded as a parametric constant not dependent on the local variable  $\mu$ . It therefore plays the role of an undetermined coefficient in this equation. Clearly, we seek only bounded solutions of this equation, since from physical considerations the deoxygenation variable is bounded above and below.

Using the initial data, we find that this equation has the bounded elementary solution

$$F_{1/2}(\mu) = \frac{bc}{\omega(ac + \xi_0^2)} \psi[1 - e^{-\omega\mu}]. \quad (33)$$

By direct substitution in Eq. 31 the unknown parametric function  $U_{1/2}(y)$  is determined as

$$U_{1/2}(y) = \frac{bc}{\xi^2(x_c, y)} \psi \left[ \frac{\xi(x_c, y)}{ac + \xi^2(x_c, y)} \right]^{1/2}. \quad (34)$$

Note that these "correction terms" influence the solution only in the "boundary-layer" near  $x = x_c$  and permit the exact satisfaction of the boundary conditions at  $x = x_c$ . We are now in a position to investigate solutions for the coupled equations (Eqs. 3) and the equilibrium solution (Eq. 16) for parameters of physiologic interest. The correction terms given by Eqs. 33 and 34, when used in the expansions (Eqs. 30) enable us to estimate the unknowns  $F(x, y)$  and  $U(y)$  correct to order  $\epsilon$ , i.e.,  $O(10^{-4})$ . Since both  $F$  and  $U$  have values between zero and one, this is sufficient accuracy, and we need not carry the expansions (Eqs. 30) to higher-order terms.

#### APPLICATIONS AND PARAMETERS

A considerable amount of experimental work has been done in an effort to determine accurate values for the properties of myoglobin in solution (24). However, its exact behavior in in vivo muscle tissues remains to be clarified. The experimental evidence suggests that the myoglobin has a linear diffusive ability in in vivo tissues and is free to change tissue position along diffusive gradients (9). Given this diffusive ability in tissues, a question arises of the nature of diffusive properties in intact functioning tissues. That is, does myoglobin passively diffuse through cell membranes, intracellular structures, and fluids within the tissue, or is it restricted to limited diffusion through only certain regions? The experimental evidence is not conclusive, but seems to support a general distribution of myoglobin, with linear diffusive properties (10). It is therefore appropriate to investigate a range of myoglobin diffusion coefficients in tissue whose absolute maximum cannot exceed the value given by the Stokes-Einstein formula  $D_m = KT/6\pi\mu_{H_2O}R_{mb} = 2.97 \times 10^{-6} \text{ cm}^2/\text{s}$ , where  $R_{mb}$  is the myoglobin molecular radius ( $11 \text{ \AA}$ ),  $\mu$  is the viscosity of water ( $0.6947 \times 10^{-2} \text{ g/cm s}$ ),  $K$  is the Boltzmann constant ( $1.38 \times 10^{-16} \text{ g cm}^2/\text{s}$ ), and  $T$  is the absolute temperature ( $310^\circ \text{ C}$ ).

The self-diffusion coefficient of myoglobin has been measured (24), and in an 18% solution is estimated as  $D_m = 0.7 \times 10^{-6} \text{ cm}^2/\text{s}$ . In a 10 g/100-ml solution, the measured value is found to be  $D_m = 1.06 \times 10^{-6} \text{ cm}^2/\text{s}$ , and in a 10% protein solution is  $\sim D_m = 2.00 \times 10^{-6} \text{ cm}^2/\text{s}$ . The protein concentration in muscle is  $\sim 18\%$ ; thus, the 18% self-diffusion value is probably the most representative of myoglobin diffusion in muscle tissue. We shall use this value as a standard reference value, and we assume that oxygenated myoglobin has the same diffusive

properties as the deoxymyoglobin, since the oxygen molecule is very small relative to the size of the deoxymyoglobin molecule, and therefore should not significantly alter its linear diffusive properties. The possible significance of oxygen transport by oxymyoglobin diffusion will be examined in the parameter range  $D_m = 0.3 \times 10^{-6}$  to  $2.7 \times 10^{-6}$  cm<sup>2</sup>/s.

The amount of myoglobin in muscle tissue has been determined (9, 10), and consists of ~1.4% of dry weight in cardiac muscle, and 2.5% of dry weight in skeletal muscle. The values for  $c_p$  considered in this study are  $c_p = 2.8 \times 10^{-7}$ ,  $5.0 \times 10^{-7}$ , and  $1.0 \times 10^{-6}$  mol/cm<sup>3</sup>. These values include those used in previous studies and represent a variation about the  $5.0 \times 10^{-7}$  reported for skeletal muscle (9). The binding properties of oxygen to myoglobin are well known (9). We shall use  $k_1 = 2.4 \times 10^7$  m<sup>-1</sup> · sec<sup>-1</sup> (on rate) and  $k_2 = 6.5 \times 10^1$  sec<sup>-1</sup> (off rate) as the kinetic parameters for the binding reaction. The equilibrium constant for this reaction is  $\kappa = k_1/k_2 = 3.7 \times 10^5$  m<sup>-1</sup>.

In cardiac muscle, the values of the myoglobin content and the tissue diffusion radius, measured from the center of the average capillary, are roughly half the corresponding skeletal muscle values. We have chosen to use skeletal muscle values as the representative parameters (21). These are taken as  $r_c = 3$  μm (capillary radius),  $r_t = 30$  μm (tissue cylinder radius), and  $z_c = 300$  μm (capillary length). The normal whole-blood characteristics are used as the properties of capillary blood:  $C = 9.107 \times 10^{-6}$  mol/mol (blood capacity for O<sub>2</sub>), and  $s_b = 1.560 \times 10^{-9}$  mol/mol (solubility of O<sub>2</sub> in whole blood). The oxygen dissociation curve for blood is computed from the Adair form  $H(P) = (P/4)(d/dP) \ln (1 + A_1P + A_2P^2 + A_3P^3 + A_4P^4)$ , where  $H$  is the saturation fraction,  $P$  is the oxygen partial pressure, and  $A_1 = 2.5670 \times 10^{-2}$ ,  $A_2 = 7.7734 \times 10^{-4}$ ,  $A_3 = 4.4700 \times 10^{-6}$ , and  $A_4 = 2.5510 \times 10^{-6}$  are the Adair constants. These values produce the normal dissociation curve and its correct slope (23). Arterial blood oxygen pressure is taken as normoxic,  $P_A = 100$  mmHg, and a blood flow velocity of  $v_o = 275$  μm/s, is used. This rate is lower than the average normal (400 μm/s) value and should produce areas of tissue hypoxia in the absence of the myoglobin. This rate enables us to examine the maximum contribution of the myoglobin to the transport process. In this study, hypoxia is taken to be the oxygen pressures below which the tissue metabolic rate would begin to decrease.

In the tissue, the parameters used are representative of the resting steady state. We have not attempted to examine the transition states; only steady-state conditions are considered. We have used  $K = 5.00 \times 10^{-8}$  mol O<sub>2</sub>/s/cm<sup>3</sup> (resting metabolic rate of skeletal muscle),  $D_o = 1.50 \times 10^{-5}$  cm<sup>2</sup>/s (diffusion rate of dissolved oxygen in skeletal muscle), and  $s_t = 1.323 \times 10^{-9}$  mol O<sub>2</sub>/vol tissue/mmHg (solubility of oxygen in skeletal muscle). These parameters will represent the tissue conditions for which a parametric examination will be conducted.

## PARAMETRIC RESULTS AND DISCUSSION

The first parametric investigation is into the nature of the nonequilibrium kinetics as predicted by the perturbation solution (Eq. 30). It was shown that the zero-order approximation to Eq. 18 produces the kinetic equilibrium solution (Eq. 16) for the tissue facilitation. The oxymyoglobin saturation fraction predicted by this solution at the capillary-tissue interface for the standard model parameters is shown as the dashed line in Fig. 3. The respective solid curves on this graph represent the oxymyoglobin fractions computed from the nonequilibrium

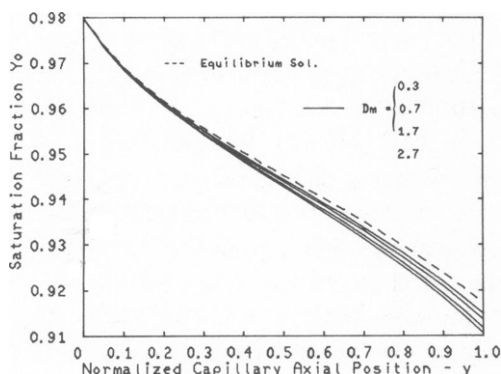


FIGURE 3

FIGURE 3 The oxymyoglobin saturation states at the capillary-tissue interface. The dashed curve represents the oxymyoglobin saturation fraction at equilibrium; the successive solid curves each represent the oxymyoglobin saturation fraction for myoglobin diffusion coefficients of 0.3, 0.7, 1.7, and  $2.7 \times 10^{-6}$ , respectively.  $D_m$ , the diffusion coefficient, is  $\times 10^6$ .  $x = 0.1$ . The myoglobin concentration is fixed at  $5.0 \times 10^{-7}$  mol/cm<sup>3</sup>.

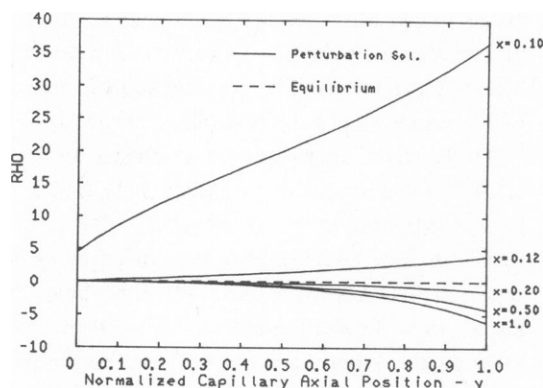


FIGURE 4

FIGURE 4 The kinetic reaction rate in distributed tissue locations. The reaction rate  $\rho(x, y)$  is computed for the standard values of the reference parameters at several fixed tissue radial positions. The solid curves represent the nonequilibrium rate of the oxygen-myoglobin binding reaction. The positive curves correspond to oxygen uptake and the negative curves represent oxygen release from oxymyoglobin.  $C_p = 5.0 \times 10^{-7}$ ,  $D_m = 0.7 \times 10^{-6}$ .

solutions for each of the myoglobin diffusion coefficients of 0.3, 0.7, 1.7,  $2.7 \times 10^{-6}$  cm<sup>2</sup>/s. As anticipated, the equilibrium solution overpredicts the nonequilibrium saturation levels, and the difference increases from arteriolar to venous end of the capillary. The differences are greater for the larger myoglobin diffusion coefficients. The monotone nature of these curves, of course, reflects the increased rate of movement of oxymyoglobin away from the boundary, due to the increase in diffusion coefficient. The kinetic equilibrium curve is unaffected by changes in the diffusion coefficient, since its values depend only on the equilibrium constant  $\kappa$  and the capillary-tissue interface oxygen pressure.

The role and importance of the system kinetics can be examined by a direct computation of the distributed reaction rate  $\rho$ ,  $\rho(x, y)$ , at various tissue locations. The question of nonequilibrium myoglobin saturation in the tissue was apparently not considered in many previous treatments. Many studies, such as (17), have assumed kinetic equilibrium of the oxymyoglobin in the tissue in order to obtain solutions of the model equations. For the model examined here, a closed-form solution is available for the kinetic equilibrium case, and the singular perturbation method permits us to examine the nonequilibrium kinetics. Thus, a distributed tissue space examination of the kinetic reaction rate can be performed.

The kinetic reaction rate,  $\rho$ , in tissue is computed for the reference parameter values and is plotted as a function of capillary axis position in Fig. 4. Each solid curve is plotted for a fixed radial position in the tissue cylinder. At  $x = 0.10$ , i.e., at  $r = r_c$ , the capillary-tissue interface, the reaction rate is everywhere positive and monotonically increasing from capillary entrance to exit. This curve shows that unsaturated myoglobin is rapidly taking up oxygen along the capillary-tissue interface. As one moves radially into the tissue, the reaction rate decreases,

but is still positive in regions of high oxygen availability. The rate drops rapidly and becomes and remains everywhere negative at about the  $x = 0.20$  radial position in the tissue region. This reflects the fact that the net kinetic mechanism is one of releasing oxygen to tissue in the tissue regions away from the capillary-tissue interface. The reaction rate takes its greatest negative value near the venous end of the tissue cylinder, where the myoglobin would be expected to make its largest contribution to oxygen supply.

The dependence of the oxymyoglobin facilitation's net value on the diffusion coefficient is displayed in Figs. 5 and 6. Fig. 5 illustrates the facilitation pressure as a function of axial position at the outermost tissue location  $x = 1.0$ , i.e.,  $r = r_t$ . The solid curves represent the kinetic equilibrium solution at the respective myoglobin diffusion coefficients, and the dashed curves are the perturbation solutions. Note that these solutions merge as the diffusion coefficient decreases. The curve at the left represents 10% of the nonfacilitated oxygen pressure, i.e.,  $P_o/10$ . For  $D_m = 0.3 \times 10^{-6}$ , the facilitation exceeds the 10% value only in the last 25% of the cylinder. Whereas, for  $D_m = 2.7 \times 10^{-6}$ , the facilitation exceeds 10% in over 65% of the cylinder. The point is that the contribution of facilitation and the importance of nonequilibrium kinetics are both quite dependent on the value of the myoglobin diffusion coefficient. The reference value of  $0.7 \times 10^{-6}$  would suggest a more than 10% augmentation of oxygen pressure in the last 40% of the cylinder's length. Note also that the contribution in each case increases almost linearly with increasing axial position.

The radial contribution of facilitation to oxygen pressure at the venous end of the tissue cylinder,  $y = 1.0$ , i.e.,  $z = z_c$ , is shown in Fig. 6. Again, the solid lines are the equilibrium

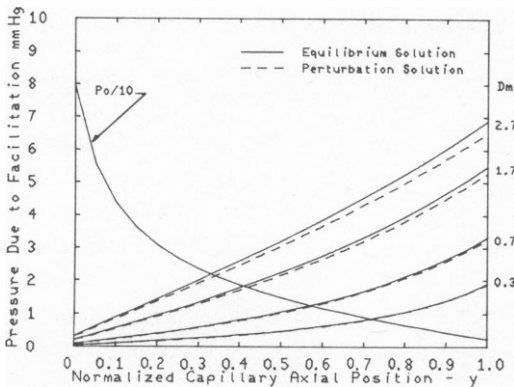


FIGURE 5

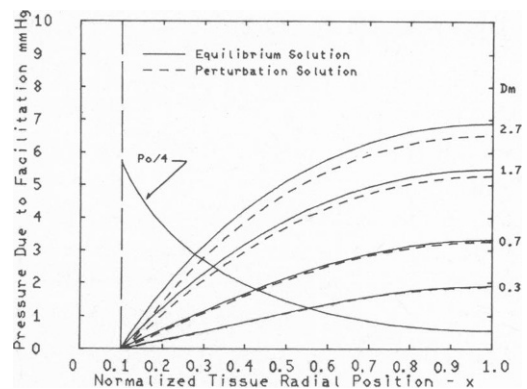


FIGURE 6

FIGURE 5 Myoglobin facilitation of oxygen transport at the limiting tissue cylinder position as a function of myoglobin diffusion coefficient. The solid curve is the equilibrium solution and the dashed curve is the nonequilibrium solution at the same value of diffusion coefficient. The facilitation is pressure ( $PO_2$ ) augmentation in millimeters of mercury (Hg). The solid curve at the left represents 10% of the nonfacilitated pressure,  $P_o(1.0, y)$ . The plot is for the outer tissue location  $x = 1.0$  as a function of the normalized axial coordinate  $y$ . The diffusion coefficient is  $D_m \times 10^{-6}$ .

FIGURE 6 Myoglobin facilitation of oxygen transport at the venous tissue cylinder position as a function of myoglobin diffusion coefficient. The solid curve is the equilibrium solution and the dashed curve is the nonequilibrium solution at the same value of diffusion coefficient. The facilitation is pressure ( $PO_2$ ) augmentation in millimeters of mercury (Hg). The solid curve at the left represents 25% of the nonfacilitated pressure,  $P_o(x, 1.0)$ . The curves are plotted for the cylinder venous location  $y = 1.0$  as a function of normalized radial coordinate  $x$ . The diffusion coefficient is  $D_m \times 10^{-6}$ .

solutions, and the dashed lines are the nonequilibrium solutions. In contrast to Fig. 5, the radial facilitation shows a parabolic shape, but the solutions again merge for the smaller values of the myoglobin diffusion coefficient. The solid curve at the left represents 25% of the nonfacilitated oxygen partial pressure, i.e.,  $P_o/4$ . In each case, this curve is exceeded within the first 60% of the tissue cylinder radius. As in Fig. 5, the results reflect a strong dependence on the magnitude of the myoglobin diffusion coefficient.

Fig. 7 illustrates the contribution of the myoglobin facilitation to the oxygen transport throughout the tissue cylinder for the reference parameter values of  $D_m = 0.7 \times 10^{-6}$ ,  $D_o = 1.5 \times 10^{-5}$ , and  $c_p = 5.0 \times 10^{-7}$ . The dashed lines are the total oxygen partial pressure,  $P_t$ , computed from the singular perturbation solution and plotted as radial pressure profiles across the tissue cylinder at 30, 50, and 100% of the capillary length. The solid line represents the radial pressure profile for no facilitation, i.e.,  $P_o$ . The greatest contribution, as one expects, is at the venous end of the capillary and in the tissue regions of lowest pressures.

Observe that in regions of high oxygen pressure, myoglobin does not release its oxygen and the facilitation does not add significantly to the total oxygen pressure. However, near the venous end of the tissue cylinder, where the pressures are nearing hypoxic values, the myoglobin facilitation becomes significant. In fact, near the venous end of the cylinder, the transport contribution by the oxymyoglobin exceeds the linear diffusion component. This suggests a possible safety mechanism against local hypoxia in muscle tissues.

The radial facilitation, as a percent of nonfacilitated pressure at the venous end, is replotted in Fig. 8. For the reference parameters, the oxymyoglobin contributes little in the first half of the tissue cylinder, exceeds 5% only in the venous half of the tissue cylinder, and for tissue radial positions that exceed  $x = 0.5$ . When the local tissue pressure nears the hypoxic levels,

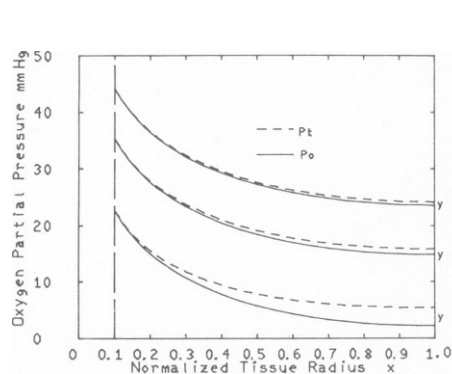


FIGURE 7

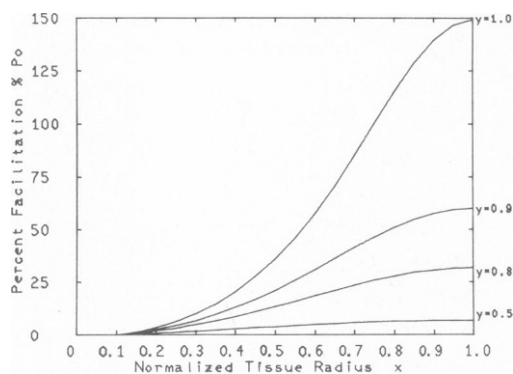


FIGURE 8

FIGURE 7 The total myoglobin contribution to tissue transport. The solid curve is nonfacilitated pressure  $P_o$  at the respective cylinder axial positions. The dashed curves are the total facilitated pressure  $P_t$  in the tissue. Note that the contribution due to facilitation is not significant in the first half of the capillary-tissue cylinder.  $C_p = 5.0 \times 10^{-7}$ ,  $D_m = 0.7 \times 10^{-6}$ .

FIGURE 8 Percent facilitation as a function of myoglobin concentration at the venous end of the tissue cylinder. The facilitation increases monotonically with the increase in myoglobin concentration. All other parameters are the standard reference values. The independent variable is normalized cylinder radius  $x$  for fixed  $y = 1.0$ . Solid lines are percent  $P_o$ .  $C_p = 5.0 \times 10^{-7}$ ,  $D_m = 0.7 \times 10^{-6}$ .



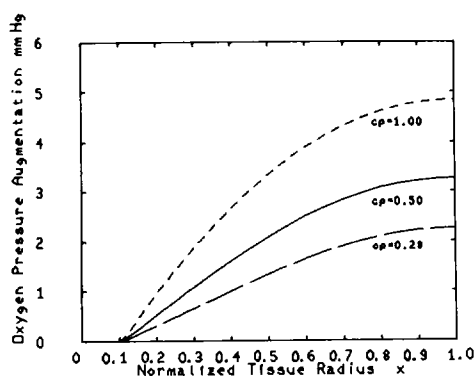


FIGURE 9 Facilitation and its contribution to total pressure levels at various myoglobin concentrations. The tissue location is the venous end of the tissue cylinder. The model parameters are the standard values with the concentration varied through the three reference values.  $C_p = \times 10^6$ ,  $\gamma = 1.00$ ,  $D_m = 0.7 \times 10^{-6}$ .

the myoglobin begins to unload its oxygen rapidly, and near the venous end, the oxygen released by the oxymyoglobin exceeds the linear diffusion transport.

Fig. 9 demonstrates the dependence of oxygen facilitation upon the tissue myoglobin concentration. The contribution to the venous region pressure is plotted in this figure for the standard value, twice the standard value, and the value used by Murray (13). The other reference parameters are held fixed. Note that the shape of the curve remains the same, but the magnitude of the oxygen facilitation is not linearly related to myoglobin concentration. No attempt has been made in this computation to compensate for diffusion coefficient changes with changing myoglobin concentration. This graph shows that the mathematical model agrees qualitatively with the experiments that have varied myoglobin tissue concentration (9).

Values of tissue oxygen pressures and oxymyoglobin saturation fractions for the reference parameters are listed in Table I. Clearly, the perturbation solution (PS) and the equilibrium solution (ES) differ significantly only near the capillary-tissue interface, and the numerical differences are less than any known pressure probe could detect. This could explain the experimental notion that oxymyoglobin is near saturation in tissue during steady-state conditions. This need not be the case in exercising muscle or in muscle undergoing periodic or transitional states (5, 9).

The fact that the reaction coefficients are quite large (i.e.,  $k_1$  and  $k_2$ ) is responsible for the nonzero net oxygen transfer rate, even though the oxymyoglobin fraction is near its saturation value. This explains how small oxymyoglobin disequilibrium can induce deoxygenation, thus unloading oxygen even when the local oxymyoglobin fraction is near the saturation value. That is, oxymyoglobin can deliver oxygen to the tissues while appearing to remain in a nearly saturated state. Oxymyoglobin can also rapidly respond to small local pressure variations within the tissue region. This property may be particularly important, since mitochondria are inhomogeneously distributed in cells and undoubtedly produce small local regions with high oxygen pressure gradients, which are seen only as average gradients across these regions. In such a case, the local oxymyoglobin could direct oxygen into these higher consumption regions

by its ability to transfer oxygen over the smaller oxymyoglobin gradients outside these regions.

## SUMMARY AND COMMENT

We have shown by our modeling studies that the facilitation role of myoglobin in muscle tissues may be one of a safety mechanism against local hypoxia and, simultaneously, a transport mechanism of some importance under more widespread hypoxic conditions. We have also shown that the assumption of kinetic equilibrium in the tissues may provide a reasonable prediction of pressure levels in the tissues, but it does not provide insight into the dynamics of the myoglobin-induced transport process. Perhaps more importantly, our studies suggest that the significant role of the myoglobin may be that of a buffer mechanism against local hypoxia. To investigate this role more completely, the steady-state models would have to be improved and expanded to include and consider transients, time-dependent flow, and metabolic rate. Such studies are beyond the scope of this investigation, but could form the basis of further modeling efforts in this area. Such efforts must necessarily include better, or more complete, experimental data on the role of myoglobin as well as the blood-tissue model structure.

The model and results discussed here are at best a crude approximation to microcirculatory structure and function. It is possible that our representation of blood and tissue invalidates the results as discussed. For example, the blood might be more nearly represented by a moving layer of hemoglobin in which facilitated radial diffusion within the capillary should be considered as well. Another possibility is that the myoglobin remains fixed at least within a single cell rather than possessing an ability to cross cell membranes. For example, Chance and associates claim to be unable to demonstrate significant facilitation in rat heart preparations, even at very low oxygen pressures.<sup>2</sup> One explanation could be that the myoglobin remains fixed in the smaller heart muscle cells and can contribute only insignificant rotational facilitation (10). If all cells retain their oxymyoglobin, then a different tissue model is required to describe the cell-cell transfer of oxygen.

A third possibility is that the true oxymyoglobin diffusion in *in vivo* tissues is smaller than the values considered here. If this is the case, then one may argue that the oxymyoglobin facilitation is insignificant. Each of these alternatives still leave us with the question, "Why is the myoglobin found in heart and striated muscle?" These alternatives all seem to require better experimental evidence and understanding before more elaborate modeling efforts can continue.

*Received for publication 17 January 1979 and in revised form 11 September 1979.*

## REFERENCES

1. ROUGHTON, R. J. W. 1932. Diffusion and chemical reaction velocity as joint factors in determining the rate of uptake of oxygen and carbon monoxide by the red blood corpuscle. *Proc. R. Soc. Lond. B. Biol. Sci.* **III**:1-36.
2. MILLIKAN, G. A. 1939. Muscle-hemoglobin. *Physiol. Rev.* **19**:503-523.
3. KLUG, A., F. KREUZER, and F. J. W. ROUGHTON. 1956. The diffusion of oxygen in concentrated hemoglobin solutions. *Helv. Physiol. Pharmacol. Acta.* **14**:121-128.

---

<sup>2</sup>Chance, B. 1979. Personal communication.

4. KLUG, A., F. KREUZER, and F. J. W. ROUGHTON. 1956. Simultaneous diffusion and chemical reaction in thin layers of hemoglobin solution. *Proc. R. Soc. Lond. B. Biol. Sci.* **145**:452-472.
5. WITTENBERG, B. A., J. B. WITTENBERG, P. R. B. CALDWELL. 1975. Role of myoglobin in the oxygen supply to red skeletal muscle. *J. Biol. Chem.* **250**:9038-9043.
6. MILLIKAN, G. A. 1937. Experiments on muscle haemoglobin in vivo; the instantaneous measurement of muscle metabolism. *Proc. R. Soc. Lond. B. Biol. Sci.* **123**:218-241.
7. WITTENBERG, J. B. 1959. Oxygen transport: a new function proposed for myoglobin. *Biol. Bull. (Woods Hole)*. **117**:402.
8. SCHOLANDER, P. F. 1960. Oxygen transport through haemoglobin solutions. *Science (Wash., D.C.)*. **131**:585-590.
9. WYMAN, J. 1966. Facilitated diffusion and the possible role of myoglobin as a transport mechanism. *J. Biol. Chem.* **241**:115.
10. WITTENBERG, J. B. 1970. Myoglobin-facilitated oxygen diffusion: role of myoglobin in oxygen entry into muscle. *Physiol. Rev.* **50**:559-636.
11. KREUZER, F. 1970. Facilitated diffusion of oxygen and its possible significance; a review. *Respir. Physiol.* **10**:686-692.
12. KREUZER, F., and L. J. C. HOOFD. 1970. Facilitated diffusion of oxygen in the presence of hemoglobin. *Respir. Physiol.* **8**:280.
13. MURRAY, J. D. 1971. On the molecular mechanism of facilitated oxygen diffusion by haemoglobin and myoglobin. *Proc. Roy. Soc. Lond. B. Biol. Sci.* **178**:95-110.
14. SMITH, K. A., J. M. MELDON, and C. K. COLTON. 1973. An analysis of carrier facilitated transport. *A.I.Ch.E. J.* **19**:102-111.
15. RUBINOW, S. I., and M. DEMBO. 1977. The facilitated diffusion of oxygen by hemoglobin and myoglobin. *Biophys. J.* **18**:29-42.
16. MURRAY, J. P. 1974. On the role of myoglobin in muscle respiration. *J. Theor. Biol.* **47**:115-126.
17. TAYLOR, B. A., and J. D., MURRAY. 1977. Effect of the rate of oxygen consumption on muscle respiration. *J. Math. Biol.* **4**:1-20.
18. VAN OUWERKERK, H. J. 1977. Facilitated diffusion in a tissue cylinder with an anoxic region. *Pflugers Arch. Eur. J. Physiol.* **372**:221-230.
19. KROGH, A. 1919. The number and distribution of capillaries in muscles with calculations of the oxygen pressure head necessary for supplying the tissue. *J. Physiol. (Lond.)*. **52**:409-415.
20. PLYLEY, M., and A. C. GROOM. 1975. Geometrical distribution of capillaries in mammalian striated muscle. *Am. J. Physiol.* **288**:1376-1383.
21. PLYLEY, M., G. SUTHERLAND, and A. C. GROOM. 1976. Geometry of the capillary network in skeletal muscle. *Microvasc. Res.* **11**:161-173, 1976.
22. FLETCHER, J. E. 1975. A model describing the unsteady transport of substrate to tissue from the microcirculation. *SIAM (Soc. Ind. Appl. Math.) J. Appl. Math.* **29**:449-480.
23. FLETCHER, J. E. 1976. Some model results on hemoglobin kinetics and its relationship to oxygen transport in blood. In *Oxygen Transport to Tissue-II*. J. Grote, D. Reneau, and G. Thews editors. Plenum Publishing Corp., New York. 251-259.
24. RIVEROS-MORENO, V., and J. B. WITTENBERG. 1972. The self-diffusion coefficients of myoglobin and haemoglobin in concentrated solution. *J. Biol. Chem.* **247**:895-901.
25. KUTCHAI, H., J. A. JACQUEZ, and F. J. MATHER. 1972. Nonequilibrium facilitated oxygen transport in hemoglobin solution. *Biophys. J.* **10**:38-54.
26. JACQUEZ, J. A., H. KUTCHAI, and E. DANIELS. 1972. Hemoglobin-facilitated diffusion of oxygen: interfacial and thickness effects. *Respir. Physiol.* **15**:166-181.

## APPENDIX I

### Boundary-Layer Analysis

In deriving Eq. 26, it was assumed that the terms

$$\epsilon \frac{1}{x} \frac{\partial}{\partial x} \left( x \frac{\partial F}{\partial x} \right) \quad (\text{I-1})$$

could be ignored in comparison to the terms on the right in Eq. 26. This assumption implies that the derivatives  $\partial^2 F / \partial x^2$  and  $\partial F / \partial x$  are of the order one,  $O(1)$ . Since the approximate solution of Eq. 26,

given by Eq. 28, satisfies the boundary conditions at  $x = 1.0$ , we expect that this assumption holds at  $x = 1.0$ , and in some neighborhood of  $x = 1.0$ . However, at  $x = x_c$ ,  $F(x, y)$  in Eq. 28 satisfies only the first of conditions (Eqs. 24), and the derivative condition at  $x = x_c$  is not satisfied. The incorrect slope of the first approximation at  $x = x_c$  suggests that in some neighborhood of  $x = x_c$ , at least one of the derivative terms in Eq. I-1 cannot be neglected. We compensate for this "local" effect by adding to the zero-order solution (Eq. 28) a higher-order term whose derivative at  $x = x_c$  can be of zero order. In other words, we correct for the condition that the zero-order solution (Eq. 28) is correct to zero order in amplitude at  $x = x_c$ , but the zero-order slope in a neighborhood of  $x = x_c$  is incorrect. The details of this procedure are as follows: Assume

$$\begin{aligned} F(x) &= F_o(x) + \epsilon^\alpha F_\alpha(x) + O(\epsilon), \\ U(y) &= U_o(y) + \epsilon^\alpha U_\alpha(y) + O(\epsilon); \end{aligned} \quad (\text{I-2})$$

where  $0 < \alpha < 1$ , is a fractional exponent to be determined. Substituting these expansions into Eq. 23, and using Eq. 26, we derive

$$\begin{aligned} \frac{\epsilon}{x} \frac{\partial}{\partial x} \left( x \frac{\partial}{\partial x} F_\alpha \right) &= [2F_o F_\alpha + a(U_\alpha F_o + U_o F_\alpha) + \xi(F_\alpha + U_\alpha)] \\ &\quad + \epsilon^\alpha (F_\alpha + U_\alpha) F_\alpha + O(\epsilon). \end{aligned} \quad (\text{I-3})$$

Clearly, we seek a solution for  $F_\alpha$  that is significant only in a neighborhood of  $x = x_c$ . Recall that  $F_o(x, y)$  satisfies the boundary condition at  $x = 1.0$ . We therefore consider the local change of variables  $\mu = (x - x_c)\epsilon^{-\alpha}$ . Then  $x = x_c + \epsilon^{-\alpha}\mu$ ;  $\partial/\partial x = (\partial/\partial\mu)\epsilon^{-\alpha}$ ; and  $\partial^2/\partial x^2 = (\partial^2/\partial\mu^2)\epsilon^{-2\alpha}$ . Using these in Eq. I-1,

$$\begin{aligned} \frac{\epsilon}{x} \frac{\partial}{\partial x} \left( x \frac{\partial F_\alpha}{\partial x} \right) &= \epsilon^{1-2\alpha} \frac{\partial^2 F_\alpha}{\partial \mu^2} + \frac{\epsilon^{1-\alpha}}{x_c + \mu\epsilon^\alpha} \frac{\partial F_\alpha}{\partial \mu} \\ &= 2F_o F_\alpha + a(U_\alpha F_o + U_o F_\alpha) \\ &\quad + \xi(F_\alpha + U_\alpha) + \epsilon^\alpha (F_\alpha + U_\alpha) F_\alpha + O(\epsilon^{1-\alpha}). \end{aligned} \quad (\text{I-4})$$

The exponents in this equation are consistent if  $\alpha = 1/2$ . Choosing  $\alpha = 1/2$ , neglecting all terms of higher than zero order, and using the properties of  $F_o$  and  $U_o$ , we obtain

$$\frac{\partial^2 F_{1/2}}{\partial \mu^2} - (aU_o + \xi)F_{1/2} = \xi U_{1/2}. \quad (\text{I-5})$$

The initial conditions are

$$\begin{aligned} F_{1/2}(0) &= 0 \\ \frac{\partial F_{1/2}}{\partial \mu}(0) &= -\frac{bc}{ac + \xi^2(x_c, y)} \psi. \end{aligned} \quad (\text{I-6})$$

The bounded solution of this initial value problem will enable us to determine  $F_{1/2}(\mu)$  and  $U_{1/2}(y)$ . These solutions are derived in the main text.

#### DEFINITIONS OF PARAMETERS

$r$	Radial coordinate from capillary center
$z$	Axial coordinate along capillary axis
$r_c$	Capillary radius

$r_t$	Outer radius of tissue cylinder
$s_b$	Solubility of oxygen in capillary blood
$s_t$	Solubility of oxygen in red muscle tissue
$P_b$	Partial pressure of oxygen in capillary blood
$P_A$	Partial pressure of oxygen in arteriolar blood
$P_t$	Partial pressure of oxygen in tissue
$v_o$	Flow velocity of whole blood in capillaries
$C$	The whole blood capacity for oxygen
$D_o$	Oxygen diffusion coefficient in tissue
$D_m$	Oxymyoglobin diffusion coefficient in tissue
$Y$	Fraction of myoglobin saturated with oxygen
$Y_o$	Fraction of interface myoglobin saturated with oxygen
$U$	$1 - Y_o$ , the fraction of interface myoglobin free of oxygen
$c_p$	Tissue concentration of myoglobin
$k_1$	Rate of association of myoglobin and oxygen
$k_2$	Rate of disassociation of oxymyoglobin
$Q(P_t)$	Respiration rate in resting muscle.
$K$	Approximate resting metabolic rate of skeletal muscle
$\alpha$	$C/s_b$
$\Omega$	$(r_t/r_c)^2 - 1$ , the constant related to area of tissue annulus
$G$	$c_p D_p / s_t D_o$ , the constant factor conversion to pressure
$\kappa$	$k_1/k_2$ , the equilibrium constant for myoglobin-oxygen
$x$	$r/r_t$ , the nondimensional radial coordinate
$x_c$	$r_c/r_t$ , the nondimensional capillary radius
$y$	$z/z_c$ , the nondimensional axial coordinate
$\epsilon$	the perturbation parameter
$a$	$\epsilon(c_p k_1 r_t^2 / D_o)$
$b$	$\epsilon(s_t k_1 r_t^2 / D_p)$
$c$	$\epsilon(k_2 r_t^2 / D_p)$
$\psi$	$[(1/x_c) - x_c] 2D_o s_t / K r_t^2$
$H(P)$	$(1/4)P(d/dP) \ln(1 + A_1 P + A_2 P^2 + A_3 P^3 + A_4 P^4)$ is the oxygen-hemoglobin dissociation function (Adair equation).

## NUMERICAL VALUES FOR CONSTANTS

### *Reference Model:*

$A_1 = 2.5670 \times 10^{-2}$
$A_2 = 7.7734 \times 10^{-4}$
$A_3 = 4.4700 \times 10^{-6}$
$A_4 = 2.5510 \times 10^{-6}$
$P_A = 100 \text{ mmHg}$
$K = 5.00 \times 10^{-8} \text{ mol O}_2/\text{s}/\text{cm}^3$
$D_o = 1.50 \times 10^{-5} \text{ cm}^2/\text{sec}$
$D_m = 0.7 \times 10^{-6}$
$v_o = 275 \text{ } \mu\text{m}/\text{s}$
$k_1 = 2.4 \times 10^7 \text{ m}^{-1} \cdot \text{s}^{-1}$ (on rate)
$k_2 = 6.5 \times 10^1 \text{ s}^{-1}$ (off rate)
$\kappa = k_1/k_2 = 3.7 \times 10^5 \text{ m}^{-1}$
$r_c = 3 \text{ } \mu\text{m}$ (capillary radius)
$r_t = 30 \text{ } \mu\text{m}$ (tissue cylinder radius)
$z_c = 300 \text{ } \mu\text{m}$ (capillary length)
$C = 9.107 \times 10^{-6} \text{ mol/mol}$ (blood capacity for $\text{O}_2$ )

$$s_b = 1.560 \times 10^{-9} \text{ mol O}_2/\text{vol blood/mmHg}$$

$$s_t = 1.323 \times 10^{-9} \text{ mol O}_2/\text{vol tissue/mmHg}$$

$$c_p = 5.0 \times 10^{-7} \text{ mol/cm}^3$$

*Parametric Ranges*

$$c_p = 2.8 \times 10^{-7}, 5.0 \times 10^{-7}, \text{ and } 1.0 \times 10^{-6} \text{ mol/cm}^3$$

$$D_m = 0.3 \times 10^{-6}, 0.7 \times 10^{-6}, 1.7 \times 10^{-6}, 2.7 \times 10^{-6} \text{ cm}^2/\text{s}$$

$$0 \leq \epsilon \leq 10^{-4}$$